Supporting Information For:

Dual Active Hf(IV)-Organic Framework for Detection of FOX-7 and Heterogeneous Catalyst on Knoevenagel Condensation

Aniruddha Das,[a] *Dhruvil Chavda,*[b, c] *Moutusi Manna,*[b, c] *Asit Kumar Das**[d]

[a]Analytical and Environmental Science Division and Centralized Instrument Facility, CSIR-Central Salt and Marine Chemicals Research Institute, Bhavnagar, Gujarat 364002, India.

[b]Applied Phycology and Biotechnology Division, CSIR Central Salt & Marine Chemicals Research Institute, Bhavnagar, Gujarat 364002, India.

[c]Academy of Scientific and Innovative Research (AcSIR), Ghaziabad 201002, India.

[d]Department of Chemistry, Krishnath College, Berhampore, Murshidabad, West Bengal, 742101, India.

*Corresponding author. Tel: +91-9706675521; +91-7001013825

E-mail address: dasaniruddha1991@gmail.com; akdas.chem@gmail.com

Materials: All the chemicals, such as Hafnium tetrachloride, 2-amino terephthalic acid, 2-hydroxy 4-methoxy benzaldehyde, sodium cyanoborohydride, formic acid, DMF, isopropanol, and various substrates used for catalysis were purchased from commercial sources and used as received.

Characterization: ^{1}H and ^{13}C NMR were recorded using a Geol resonance ECZ600R spectrometer at 25 °C. TMS was used as an internal reference during the NMR spectroscopic study. Parkin Elmer 883 spectrometer was used to record the FT-IR data using a KBr pellet. The following indications were used to indicate the corresponding absorption bands: very strong (vs), strong (s), medium (m), weak (w), shoulder (sh), and broad (br). Cu-Kα radiation was used to carry out the XRPD study, and data was recorded over a 2Θ range of 5-50 °. Thermogravimetric analyses (TGA) were carried out using an SDT Q600 thermo gravimetric analyser in the temperature range of 25-700 °C under an argon atmosphere at a heating rate of 10 °C min-1. Nitrogen sorption isotherms were recorded on a Quantachrome Autosorb iQMP gas sorption analyser at -196 °C. X-ray photoelectron spectra (XPS) were obtained from a Thermo Fischer Scientific ESCALAB XI+ using an Al Kα (hν = 1486.6 eV) X-ray source with a base vacuum operated at 300 W. JEOL JSM-7100F instrument working at 18 kV accelerating voltage was used to record the FE-SEM data. Before taking the FE-SEM images, the thin coating of Au (~ 4 nm) was coated using a vacuum evaporator. An Edinburgh Instrument Life-Spec II equipment was used to measure the fluorescence lifetimes by employing a time-correlated single-photon counting (TCSPC) procedure. UV-vis spectra in the region 250–800 nm was recorded using a Perkin Elmer Lambda 25 UV-vis spectrometer. All solutions for the UV-vis measurements were prepared by using Milli-Q water.

Synthetic protocol of MOF CSMCRI-KNC.

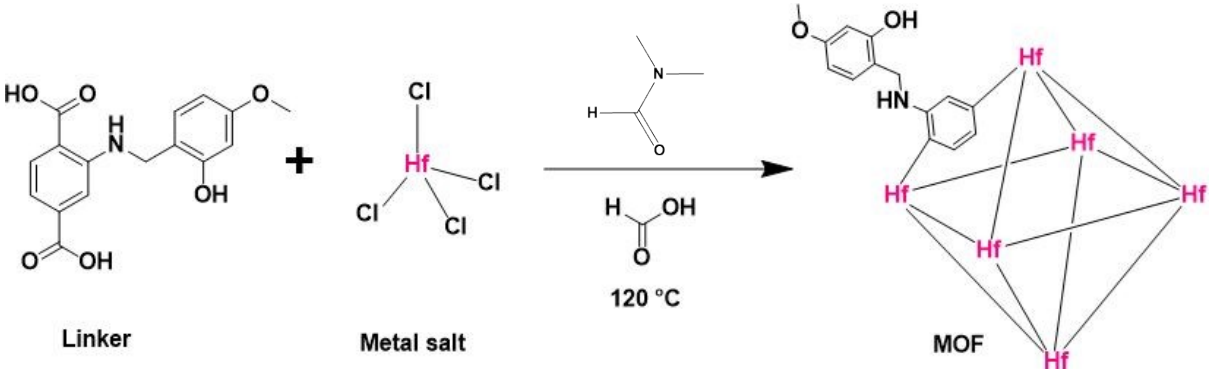

Scheme S1. Schematic presentation of synthesis of MOF **CSMCRI-KNC**.

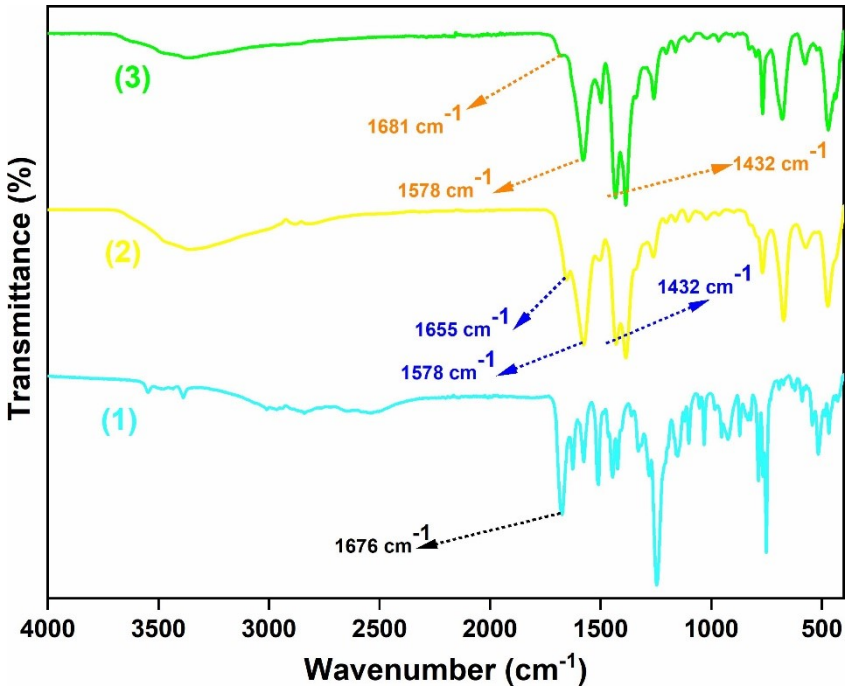

Fig. S1. FT-IR spectra of (1) H_2BDC-NH-CH_2-Ph-2OH-4OCH_3 linker, (2) as-synthesized **CSMCRI-KNC**, and (3) **CSMCRI-KNC′**.

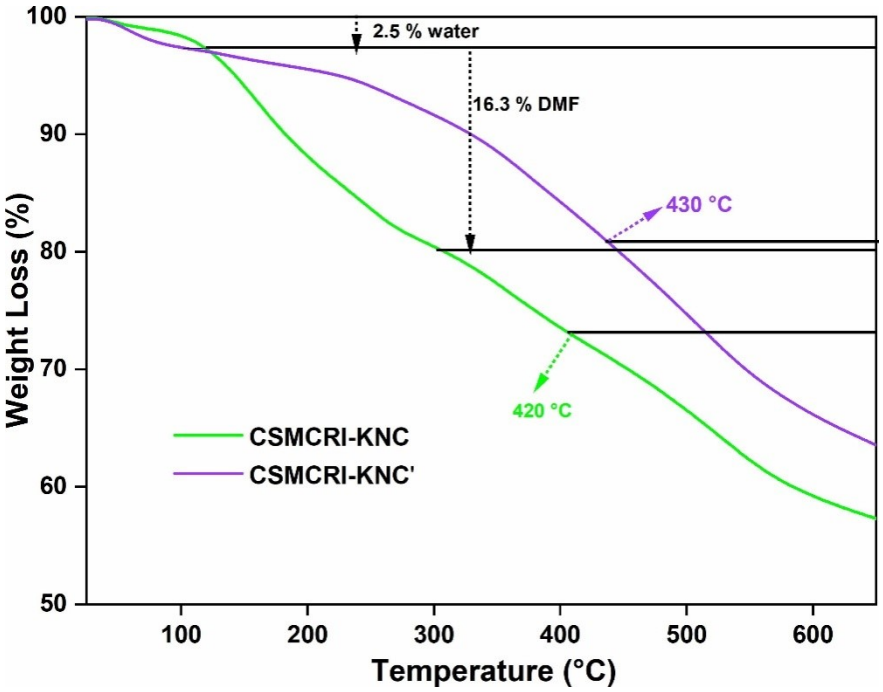

Fig. S2. TG curves of as-synthesized **CSMCRI-KNC** (green) and **CSMCRI-KNC′** (violet) recorded in an N_2 atmosphere in the temperature range of 30-650 °C with a heating rate of 5 °C min^{-1}.

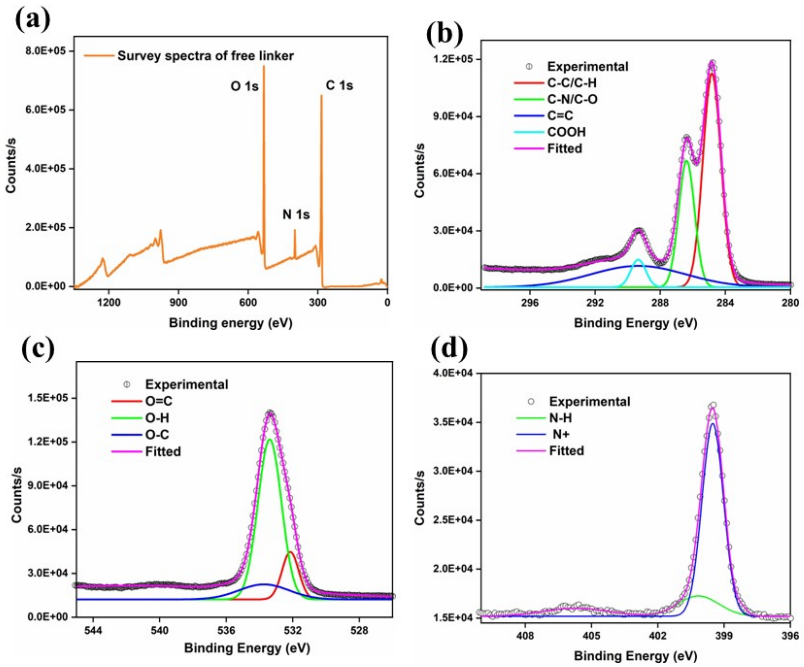

Fig. S3. The survey XPS spectrum (a) and deconvoluted XPS pattern of (b) C1s, (c) O1s, and (d) N1s in free linker.

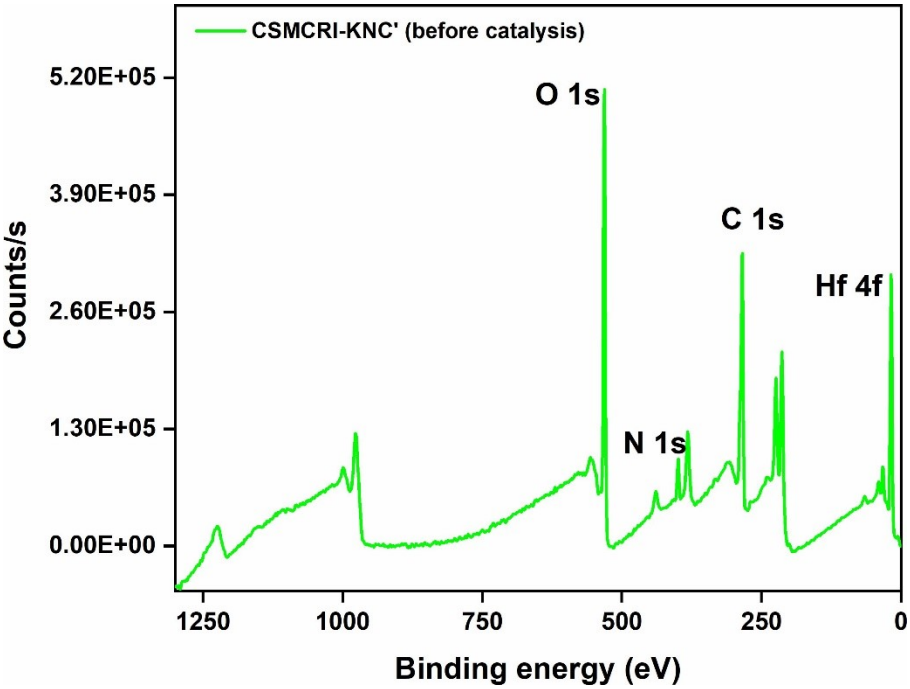

Fig. S4. X-ray photoelectron survey spectra of MOF (before catalysis) showing the presence of O 1s, N 1s and C 1s spectra at their corresponding binding energies.

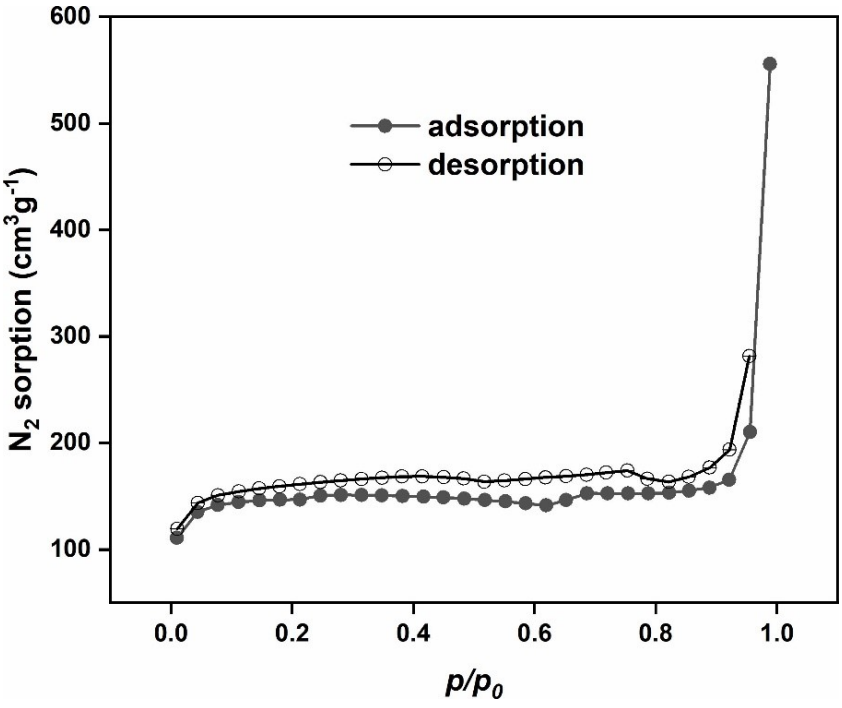

Fig. S5. N_2 sorption curve of **CSMCRI-KNC′** MOF performed at -196 °C.

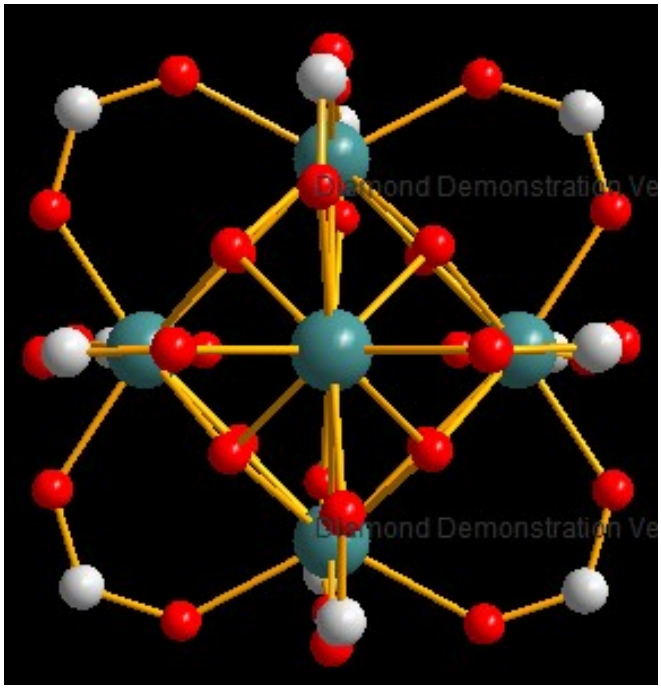

Fig. S6. Ball-and-stick representation of the framework structure of **CSMCRI-KNC′** SBU having formula $[Hf_6O_4(OH)_4]^{12+}$. Colour codes: Hf, deep cyan; C, white gray; O, red. Hydrogen atoms have been removed from the structural plots for clarity.

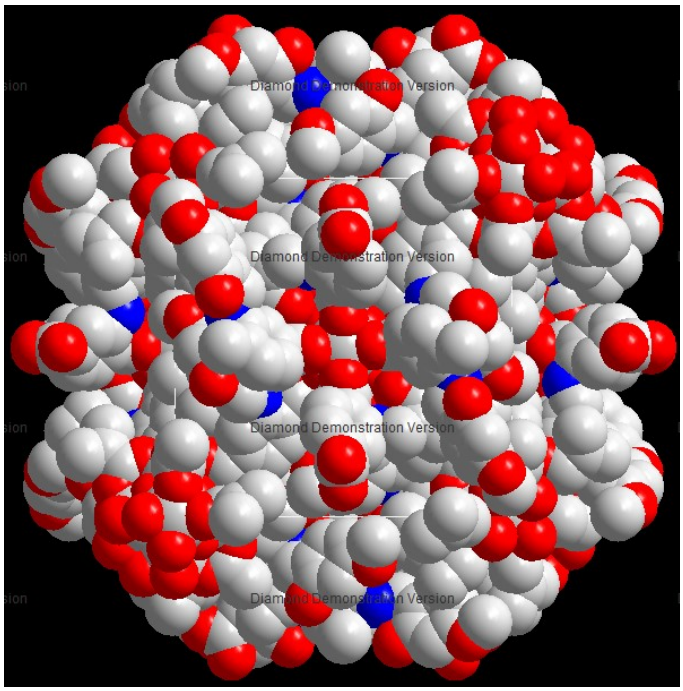

Fig. S7. Space filled representation of the framework structure of **CSMCRI-KNC′** in face-centred cubic (fcc) packing Colour codes: C, white gray; O, red. N, blue; Hydrogen atoms have been removed from the structural plots for clarity.

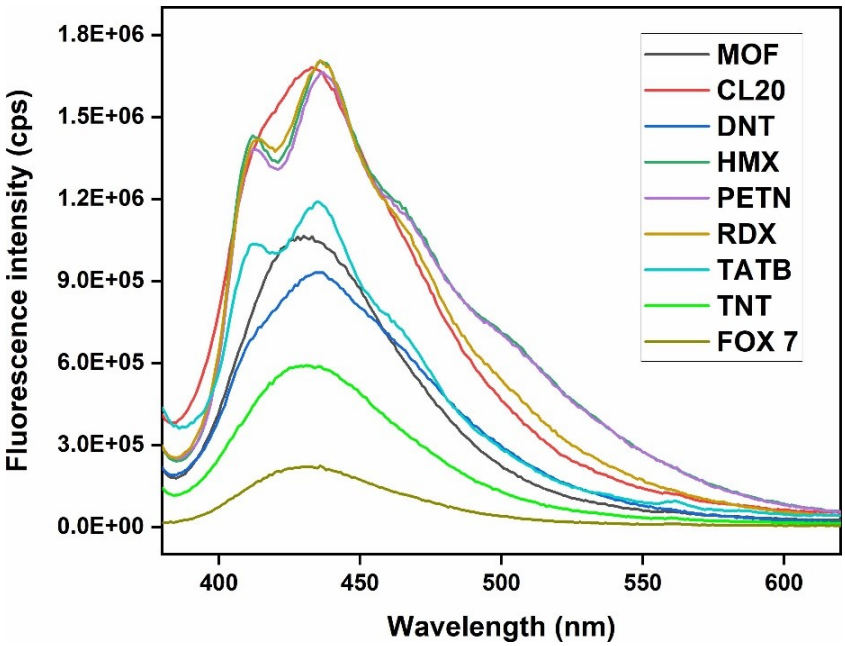

Fig. S8. Quenching of fluorescence response of MOF **CSMCRI-KNC'** in addition to (10 mM, 160 µL) various analytes in aqueous media.

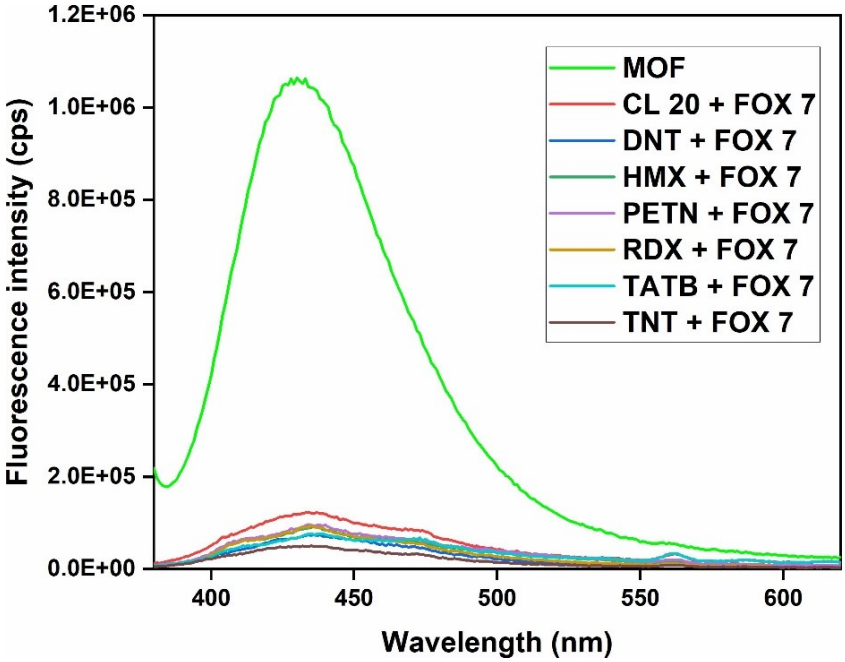

Fig. S9. Quenching of fluorescence response of MOF **CSMCRI-KNC'** in addition to (10 mM, 160 µL) FOX-7 in presence of (10 mM, 160 µL) various competitive analytes in aqueous media.

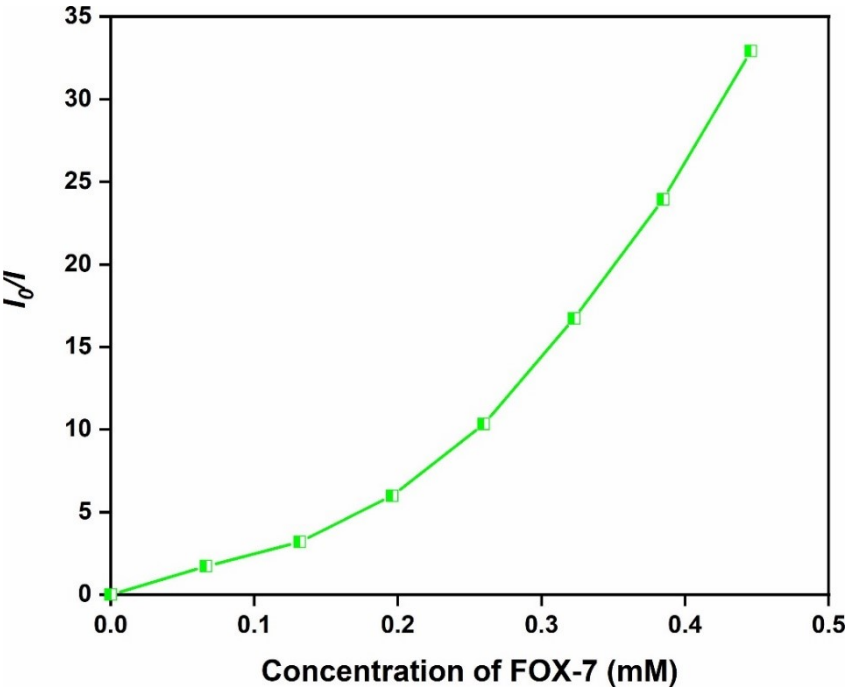

Fig. S10. Stern-Volmer plot for MOF **CSMCRI-KNC'** at high concentration of FOX-7.

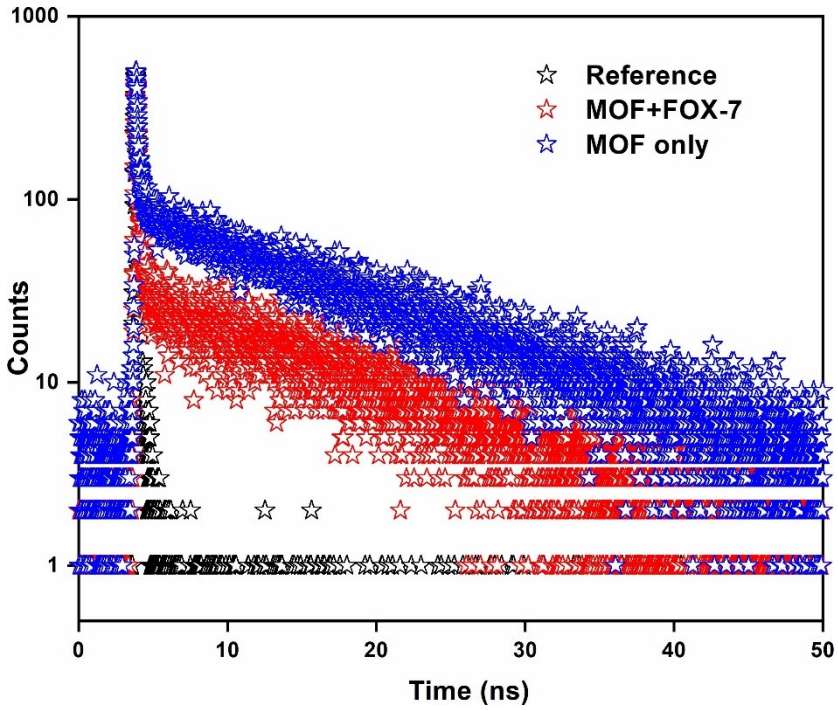

Fig. S11. Time-resolved fluorescence lifetime decay profile of **CSMCRI-KNC'** before and after addition FOX-7 in water medium.

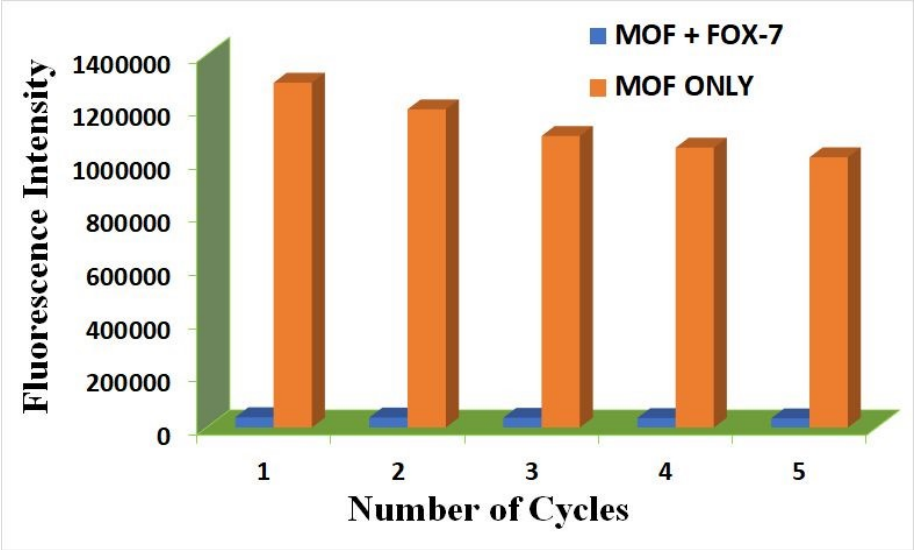

Fig. S12. The recyclability performances of f **CSMCRI-KNC'** towards FOX-7 detection in water medium.

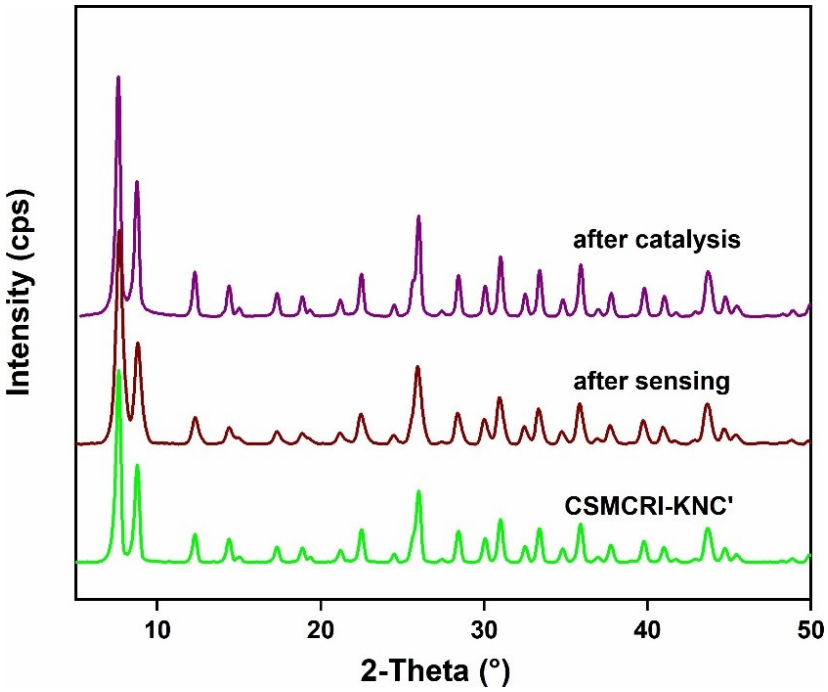

Fig. S13. XRPD patterns of the (red) simulated Hf-UiO-66, (blue) as-synthesized **CSMCRI-KNC** and (black) **CSMCRI-KNC′**.

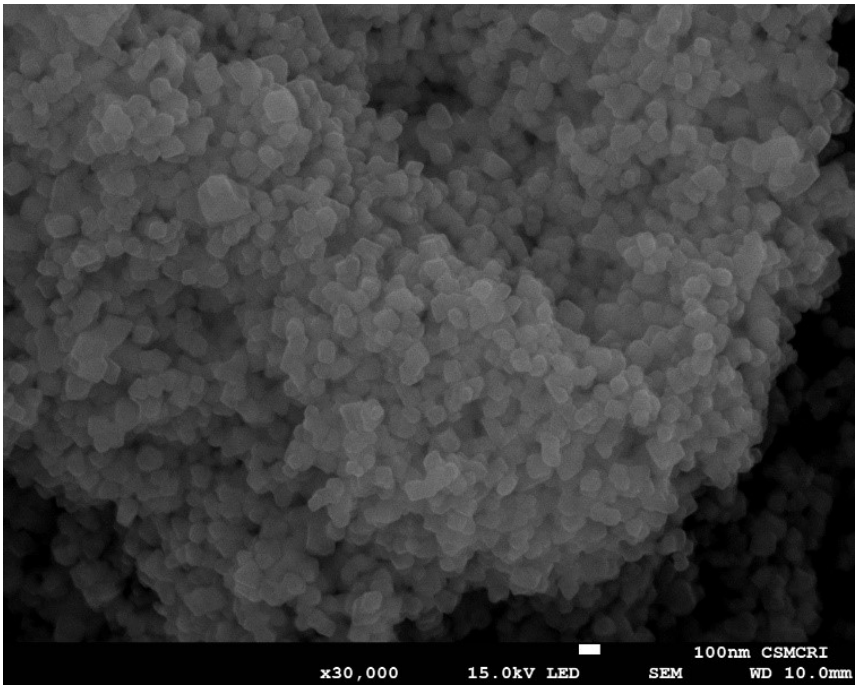

Fig. S14. FE-SEM analysis of MOF **CSMCRI-KNC'**.

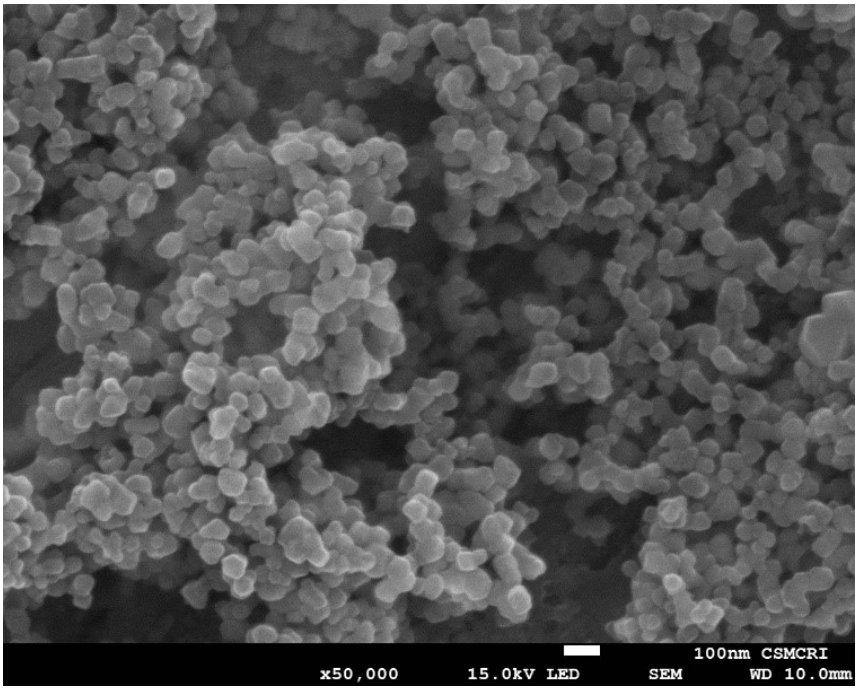

Fig. S15. FE-SEM analysis of MOF **CSMCRI-KNC'** after FOX-7 detection.

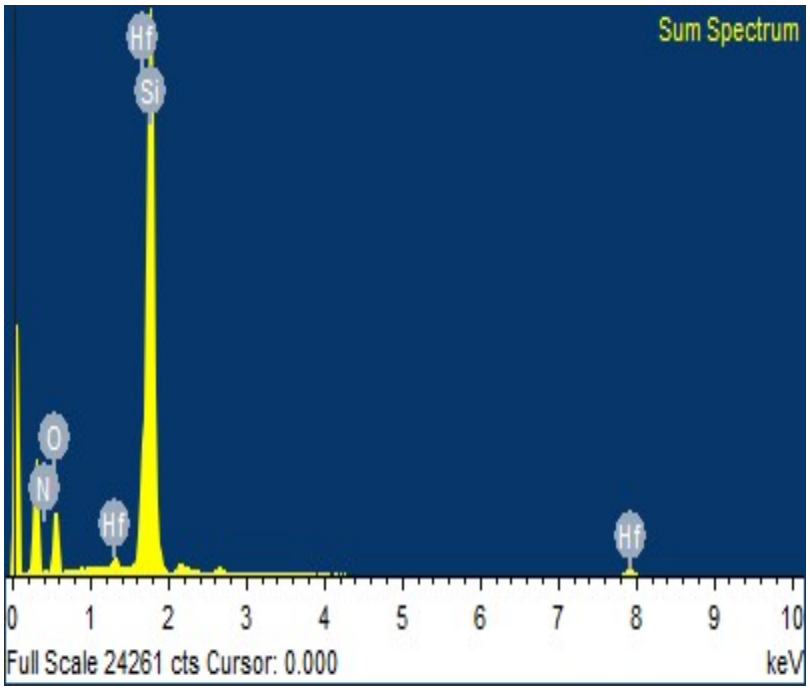

Fig. S16. EDX spectrum of MOF **CSMCRI-KNC'** before FOX-7 detection.

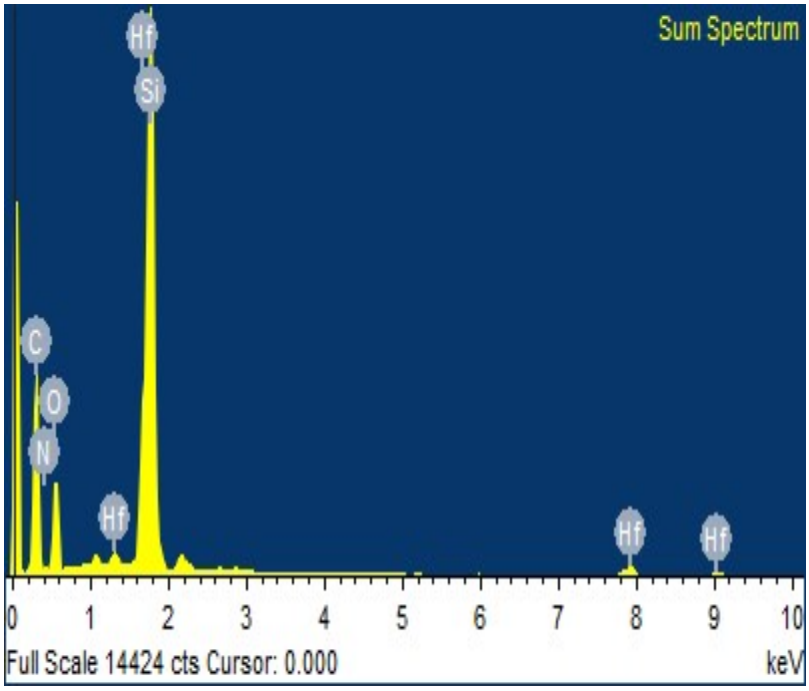

Fig. S17. EDX spectrum of MOF **CSMCRI-KNC'** after FOX-7 detection.

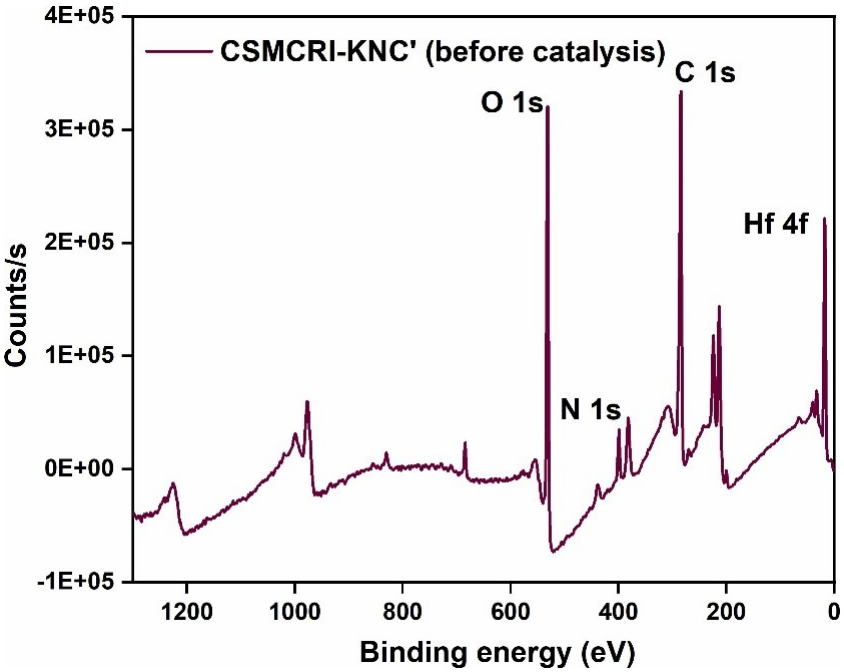

Fig. S18. X-ray photoelectron survey spectra of MOF (after sensing) showing the presence of C1s, O 1s, N 1s, and Hf 4f spectra at their corresponding binding energies.

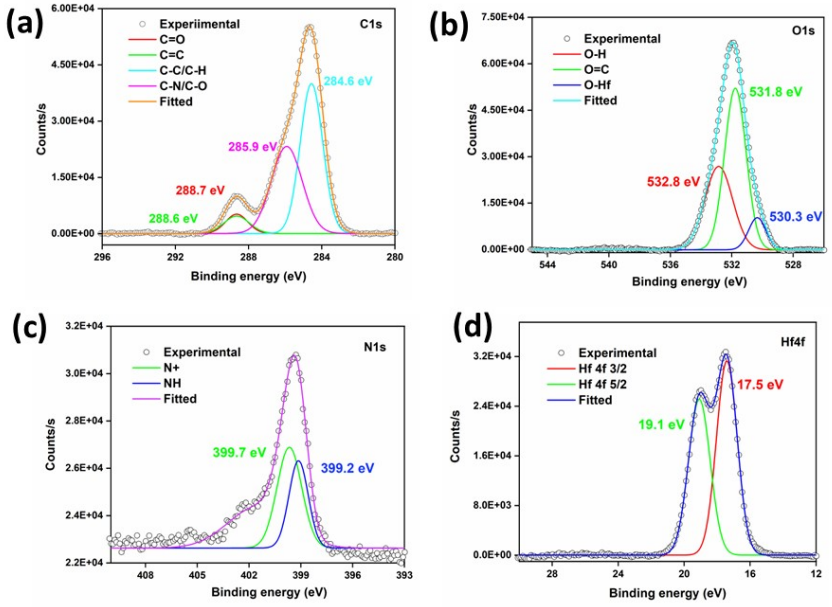

Fig. S19. The (a) deconvoluted XPS pattern of (b) C1s, (c) O1s, and (d) N1s and (d) Hf 4f in FOX-7 treated MOF.

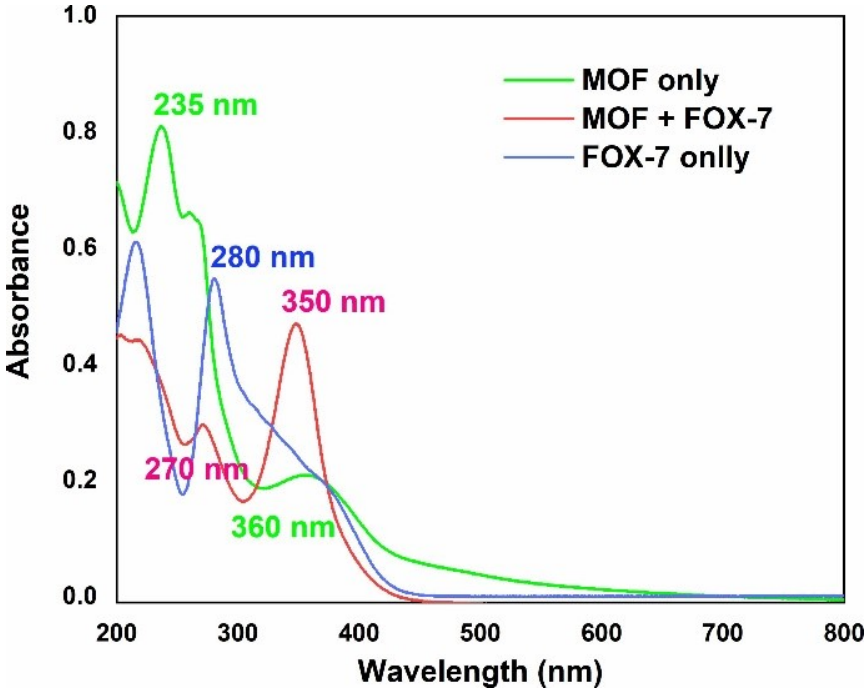

Fig. S20. The excitation spectra of only **CSMCRI-KNC´**, only FOX-7 and the FOX-7 treated **CSMCRI-KNC´**.

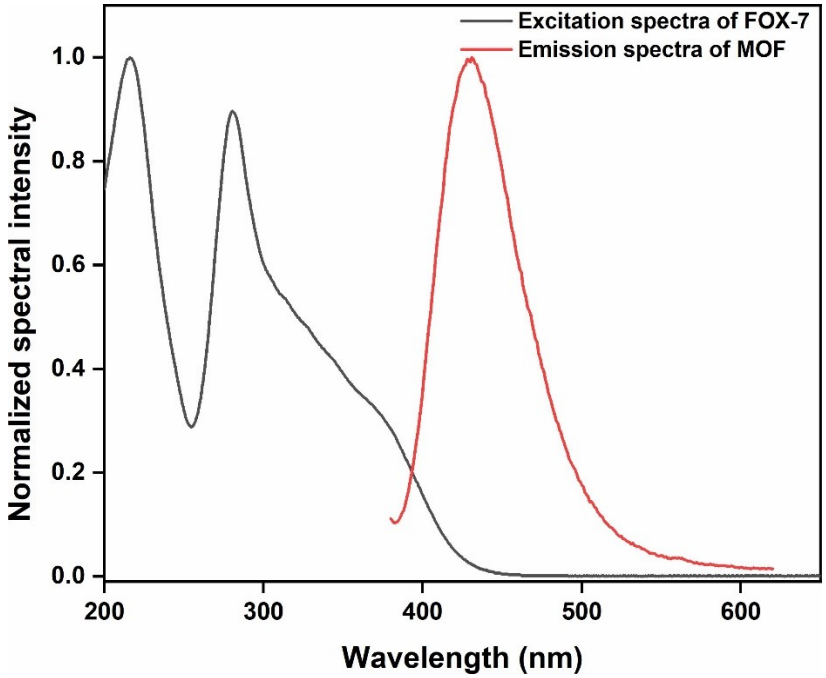

Fig. S21. The excitation spectrum of FOX-7 and the emission spectrum of only **CSMCRI-KNC´**.

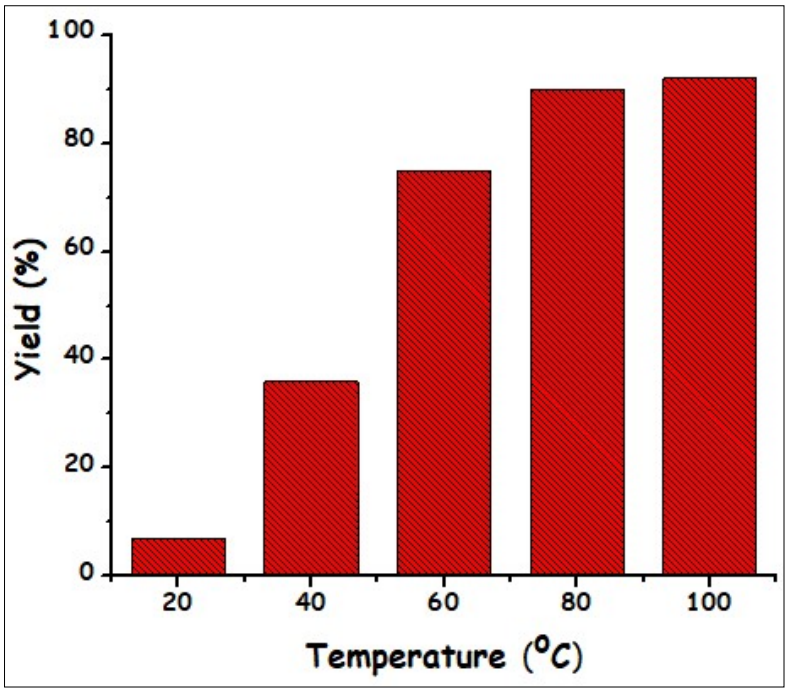

Fig. S22. Effect of temperature for the Knoevenagel Condensationreaction of barbituric acid (**1a**) (1 mmol) with 4-methylbenzaldehyde (**2a**) (1 mmol) in EtOH.

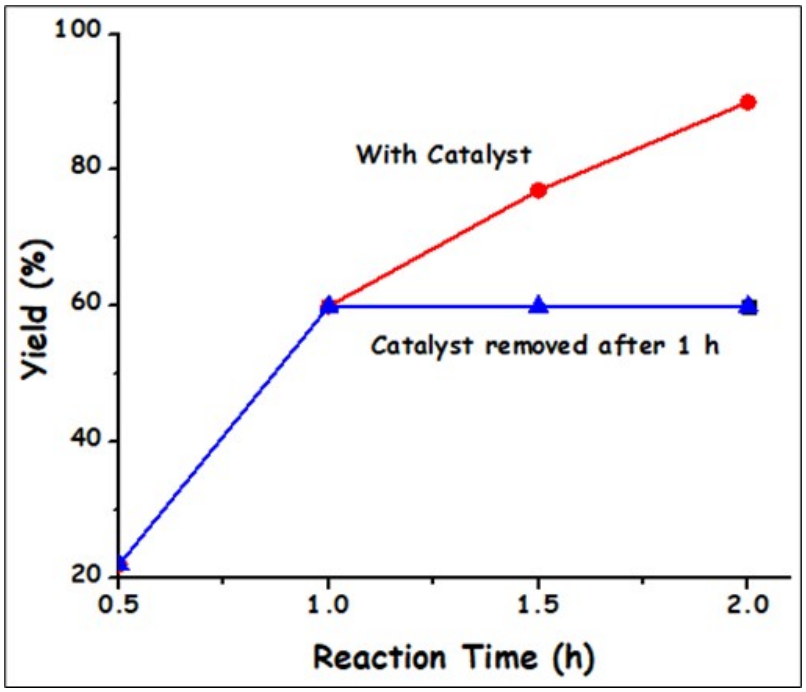

Fig. S23. Effect of reaction time for the Knoevenagel Condensationreaction of barbituric acid (**1a**) (1 mmol) with 4-methylbenzaldehyde (**2a**) (1 mmol) in EtOH in presence (red) and absence (blue) of catalyst.

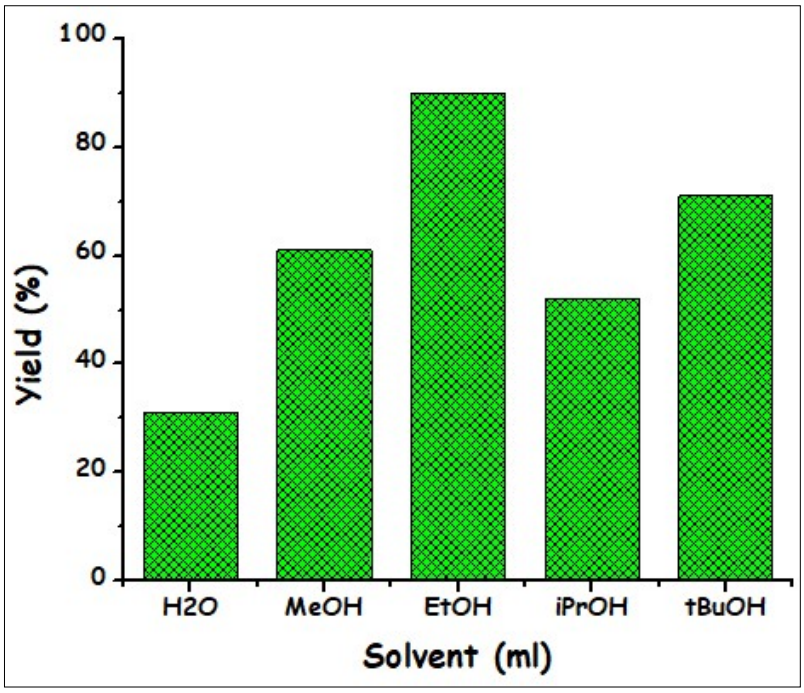

Fig. S24.Effect of solvent for the Knoevenagel Condensationreaction of barbituric acid (**1a**) (1 mmol) with 4-methylbenzaldehyde (**2a**) (1 mmol) 80 °C.

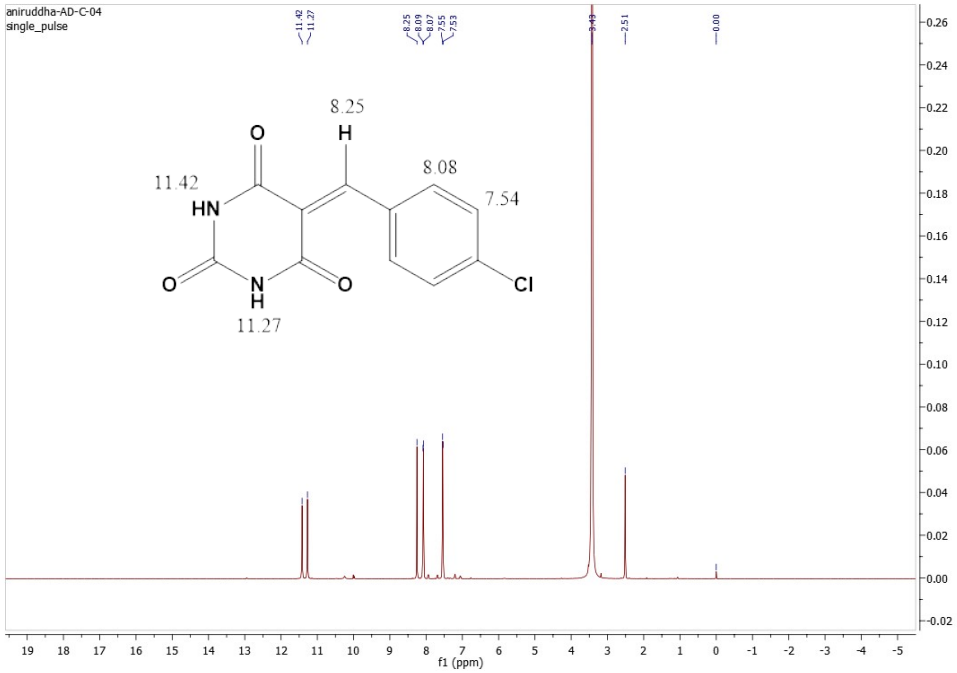

Fig. S25. ^{1}H NMR spectrum of compound 3f.

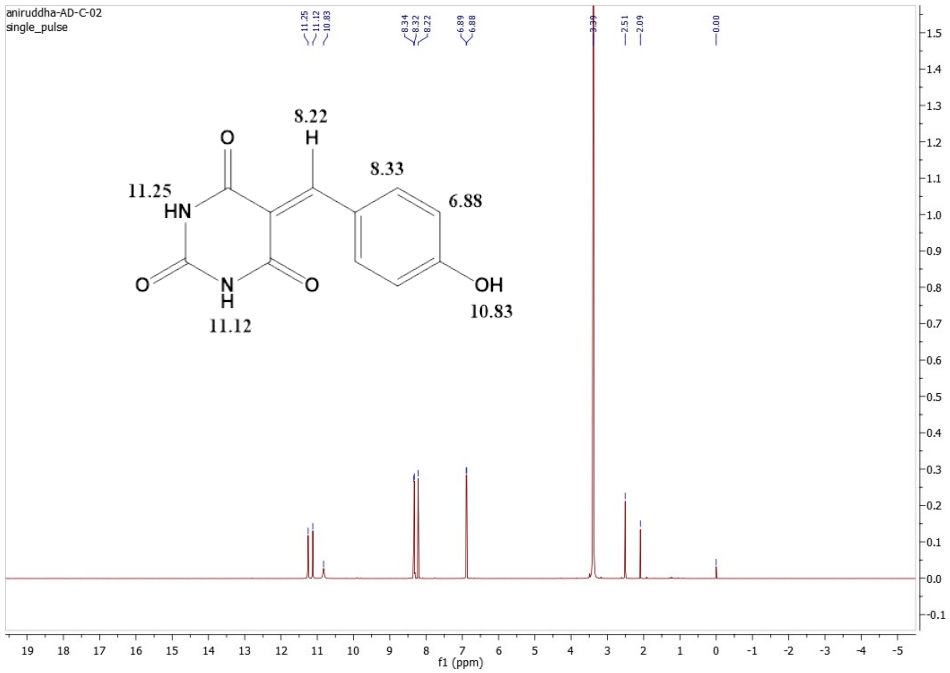

Fig. S26. ^{1}H NMR spectrum of compound 3j.

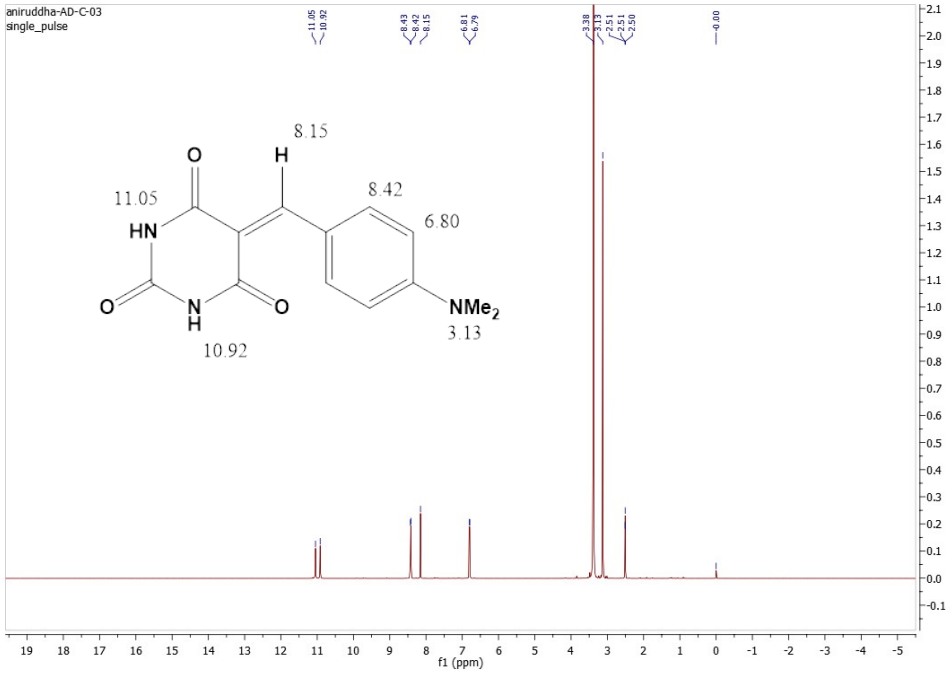

Fig. S27. ^{1}H NMR spectrum of compound 3k.

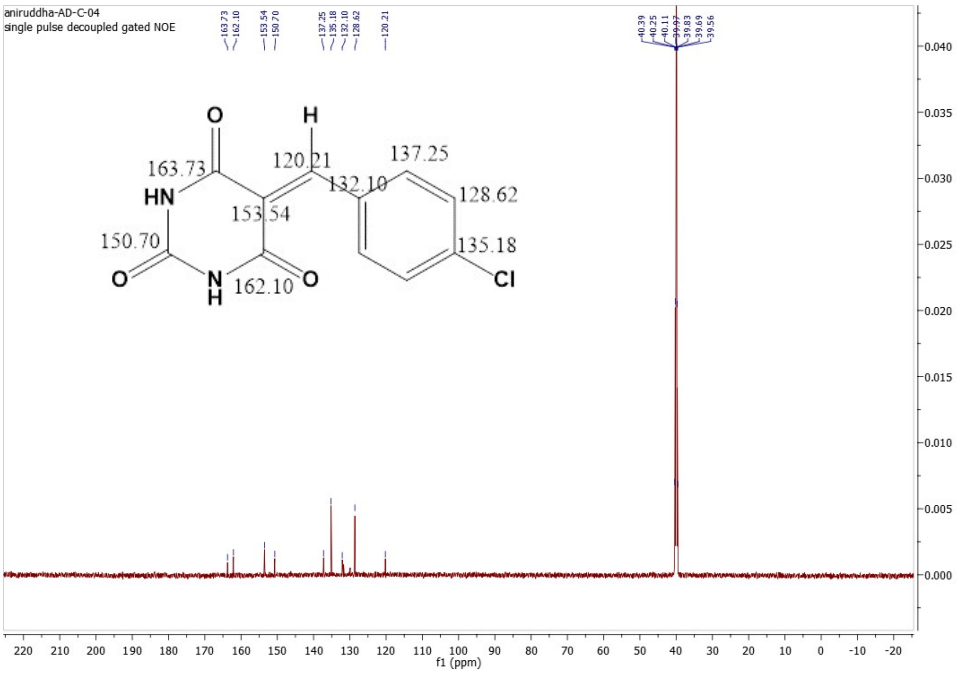

Fig. S28. ^{13}C NMR spectrum of compound 3f.

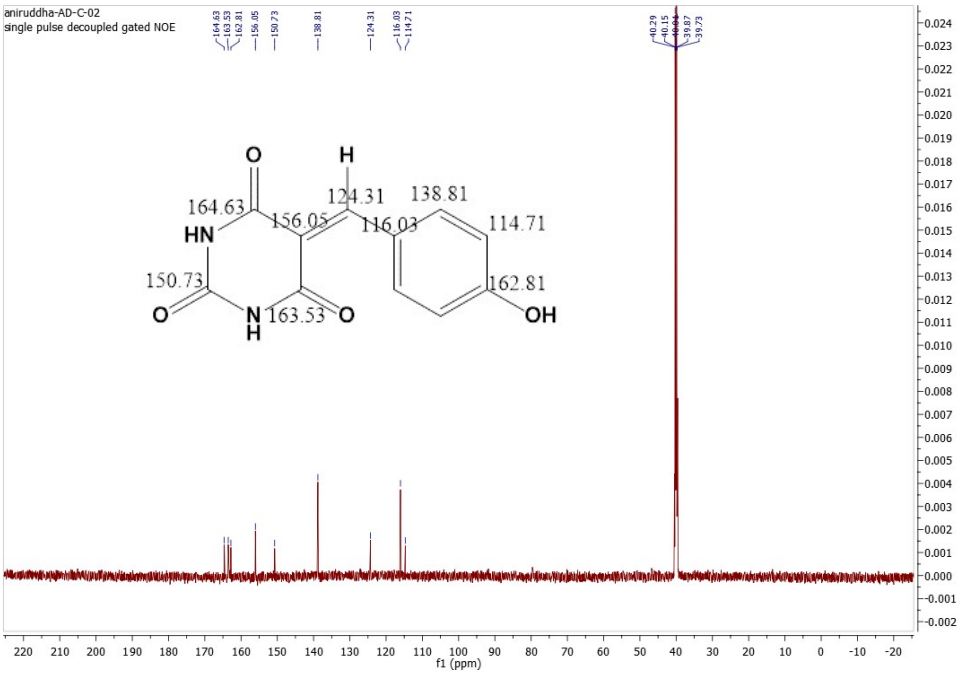

Fig. S29. ^{13}C NMR spectrum of compound 3j.

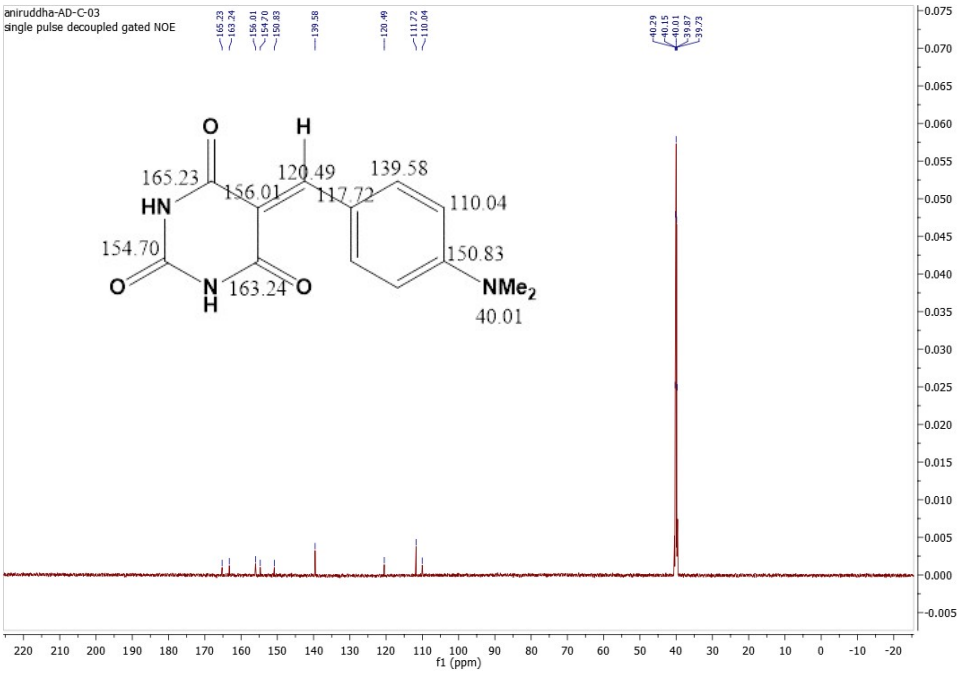

Fig. S30. ^{13}C NMR spectrum of compound 3k.

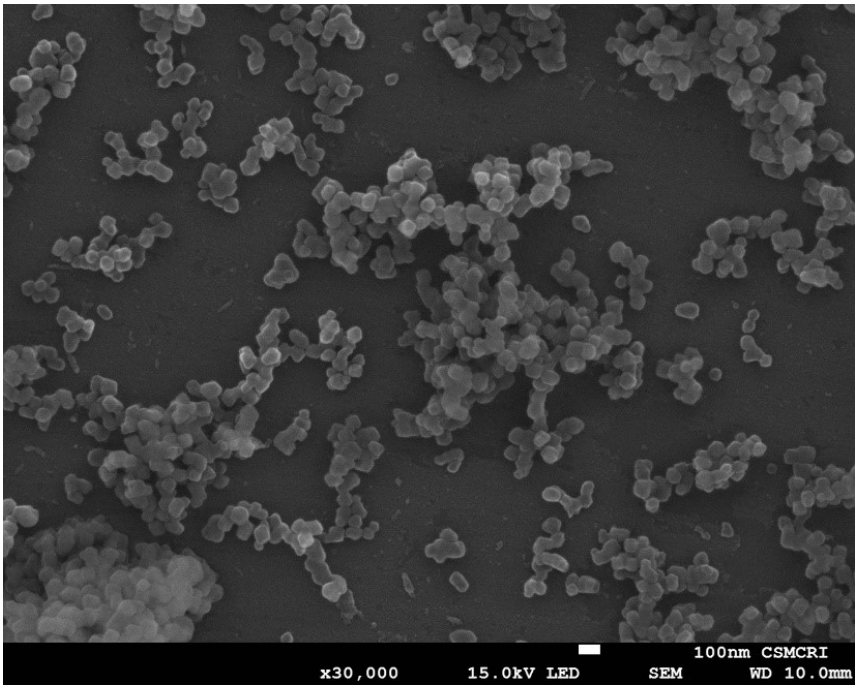

Fig. S31. FE-SEM analysis of MOF **CSMCRI-KNC'** after catalysis.

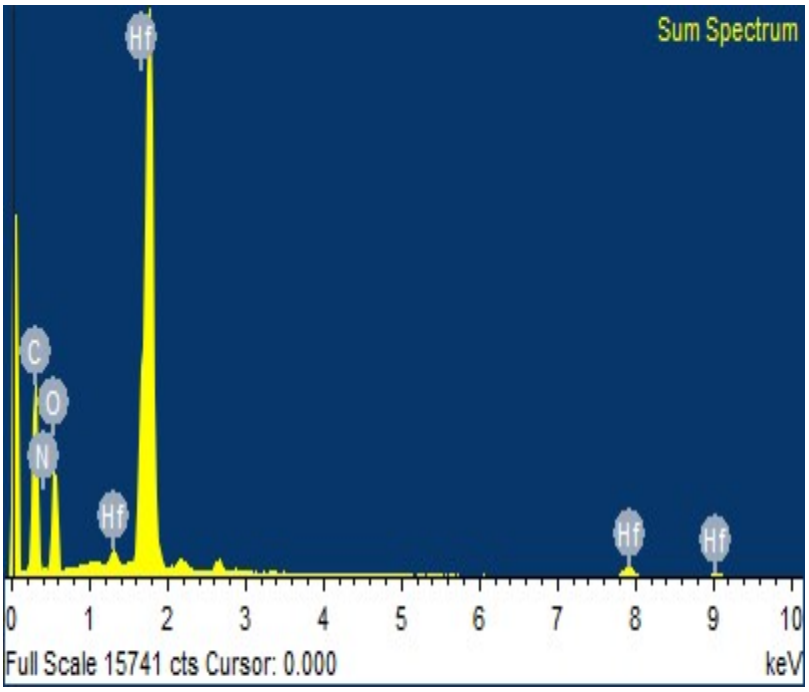

Fig. S32. FE-SEM analysis of MOF **CSMCRI-KNC'** after catalysis.

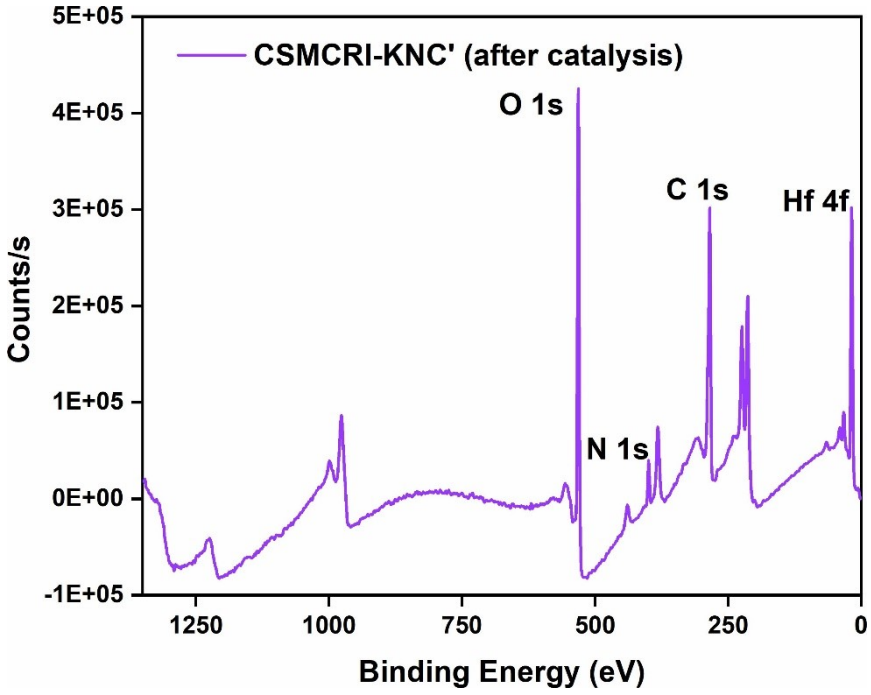

Fig. S33. X-ray photoelectron survey spectra of MOF (after catalysis) showing the presence of O 1s, N 1s and C 1s spectra at their corresponding binding energies.

Table S1. Comparison of the detection limit, response time, nature of fluorescence change, and solvent system used for FOX-7 detection for probes reported to date.

Entry	Name of probe	Detection Limit	Response Time (s)	Medium Used	Nature of Fluorescence	Ref.
1	**CSMCRI-KNC′**	189	20	water	Turn-off	This work
2	L·Eu	17	91	acetonitrile	Turn-off	1
3	L·Tb	22	84	acetonitrile	Turn-off	1
4	AM-8-Tb	218	not available	acetonitrile	Turn-off	2
5	AM-8-Eu	205	not available	acetonitrile	Turn-off	2
6	AM-8-Zn	77	not available	acetonitrile	Turn-off	2

Table S2. Average excited-state lifetime (<τ>) values of **CSMCRI-KNC′** before and after addition of 160 μL of 0.21 (M) FOX-7 solution (λex = 336 nm).

Volume of FOX-7 solution added (μL)	B_1	B_2	a_1	a_2	τ_1 (ns)	τ_2 (ns)	<τ>* (ns)	χ^2
0	0.03	0.96	1.23	0.85	0.34	14.85	13.04	1.09
160	0.13	0.86	1.89	0.24	0.25	12.31	3.42	1.15

$\langle\tau\rangle^* = a_1 \tau_1 + a_2 \tau_2$

Table S3. Comparison table of catalytic performance in terms of TON (turnover) of the presented **CSMCRI-KNC′** catalyst with other reported catalysts.

Entry	Ph-CHO (mmol)	$CH_2(CN)_2$ (mmol)	Catalyst	Temp. (° C)	Time (minutes)	Yield (%)	TON	Ref.
1	1.0	1.0	Cu-MOF (LOCOM-1) (0.04 mmol)	r.t	360	98	2462	3

2	10	20	JNU-402-NH_2 (0.04 mmol)	80 °C	60	99	1665	4
3	2.1	2.0	Cd-MOF (0.08 mmol)	r.t	720	98	1225	5
4	10	20	NUC-54a (0.3 mol%)	60 °C	300	98	327	6
5	1.0	1.1	$(Zn(ADA)(L)]\cdot 2H_2O)_n$ (1.0 mol%)	r.t	60	99	99	7
6	1.0	1.1	$[Cd(DDIH)_2H_2O]_n$ (3.0 mol%)	r.t	15	96	32	8
7	1.0	1.0*	**CSMCRI-KNC'** (0.005 mmol)	80 ° C	120	89	189	This work

*Barbituric acid (1.0 mmol) was used instead of malononitrile.

References.

1. T. S. Mahapatra, A. Dey, H. Singh, S. S. Hossain, A. K. Mandal and A. Das, *Chem. Sci.*, 1032-1042, **11**, 2020.
2. V. R. Ramlal, A. Singh, A. Das, R. Lo and A. K. Mandal, *Sens. Actuators, B*, 2024, **409**, 135551-135558.
3. S. Afaq, M. U. Akram, W. M. A. Malik, M. Ismail, A. Ghafoor, M. Ibrahim, M. Nisa, M. N. Ashiq, F. Verpoort and A. H. Chughtai, *ACS Omega*, 2023, **8**, 6638-6649.
4. G. Q. Huang, J. Chen, Y. L. Huang, K. Wu, D. Luo, J. K. Jin, J. Zheng, S. H. Xu and W. Lu, *Inorg. Chem.*, 2022, **61**, 8339–8348.
5. S. Hasegawa, S. Horike, R. Matsuda, S. Furukawa, K. Mochizuki, Y. Kinoshita and S. Kitagawa, *J. Am. Chem. Soc.*, 2007, **129**, 2607-2614.
6. H. Chen, T. Zhang, S. Liu, H. Lv, L. Fan and X. Zhang, *Inorg. Chem.*, 2022, **61**, 11949-11958.
7. B. Parmar, P. Patel, V. Murali, Y. Rachuri, R. I. Kureshy, N.-u. H. Khan and E. Suresh, *Inorg. Chem. Front.*, 2018, **5**, 2630-2640.
8. L. Tom and M. A. Kurup, *J. Solid State Chem.*, 2021, **294**, 121846.